Preparation of a composite of Cu:ZnO and the study of its structural and optical properties

Saif Dakhil Madhloom
jajsbsba158@gmail.com
Ministry of Education , Wasit Education Directorate, Wasit

تحضير مركب من النحاس و أوكسيد الزنك ودراسة خصائصه التركيبية و البصرية

م.م. سيف داخل مظلوم
وزارة التربية، مديرية تربية واسط

Abstract

The study aims to prepare nanoparticles of zinc oxide (ZnO), and add copper (Cu) to improve some of its physical properties. The structural and optical properties were studied X-ray diffraction (XRD) was used to study the crystal structure of the samples and the levels of crystalline peaks and atomic force microscopy (AFM) to examine the effect of Cu on the structural properties. The films formed as polycrystalline and the results showed that it was possible to create nanostructures with medium grain sizes.

Keywords

Nanoparticles, Pulse laser deposition , Copper , Zinc oxide.

الخلاصة

تهدف الدراسة إلى تحضير جسيمات نانوية لأوكسيد الزنك (ZnO) وإضافة النحاس (Cu) لتحسين بعض خواصه الفيزيائية. تمت دراسة الخصائص التركيبية والبصرية حيث تم استخدام حيود الأشعة السينية (XRD) لدراسة التركيب البلوري للعينات ومستويات القمم البلورية ومجهر القوة الذرية (AFM) لفحص تأثير النحاس على الخصائص التركيبية. لوحظت الاغشية التي تشكلت على أنها متعددة البلورات و أظهرت النتائج أنه كان من الممكن إنشاء تراكيب نانوية ذات أحجام حبيبات متوسطة.

Introduction

Most of the earth's crust consists of oxides. Oxides are formed from the interaction of elements with air. An oxide is a chemical reaction involving oxygen and another element. Some oxides have many properties, such as zinc oxide (ZnO) is regarded as a crucial semiconductor component because of its physical and basic characteristics[1]. There have referred to and used as a top material for potential candidates uses in photovoltaic devices and medical applications, a gas sensor, and light-emitting diodes [2]. Recently, ZnO has been the primary focus of due to its unique qualities, which make it an extremely fascinating subject for both theoretical and practical research. The relatively broad 3.37 eV band-gap at ambient temperature, one of the intriguing characteristics of the n-type ZnO semiconductor, but just one of several. This makes it suitable for use in a variety of optical applications [3,4]. Furthermore, the 60 meV exciton binding energy of ZnO is remarkable. It is characterized as one of the most important minerals used in many applications .This significant value is highly intriguing because it aids in the creation of several optoelectronic devices[5]. Specifically, a result of excitonic recombination processes, particularly sharp emission peaks are seen the photoluminescent spectrum of zinc oxide , Applications for these kinds of emissions include tunable UV photodetectors and UV excitonic lasers., as well as light-emitting diodes. According to their emission energy, other identified excitonic peaks can also be separated [6]. As a result, surface excitonic processes and bulk exitonic processes may both be observed and distinguished from free excitons and bound excitons [7]. It's interesting to note that ZnO has been shown to be exceptionally thermally stable and to have a high carrier mobility at room temperature. Reports claim that ZnO exhibits respectable pyroelectricity and piezoelectricity capabilities [8]. Additionally, ZnO has high electrical conductivity and a visible spectrum with good transparency, To enhance their optical and electrical properties, thin films of ZnO are typically doped and co-doped with a variety of suitable dopants [9].

Experimental Work

In this work, Cu: ZnO nanoparticles are created using pulse laser deposition (PLD) explain in preference to the process that was carried out to prepare the samples used in the research. PLD it is considered one the best methods for making films due to its advantages. It is superior to many other sedimentation methods. targets were eliminated employing a laser of wavelength = 1064 nm and number (500) of shots at a repetition rate of 6 Hz while using the Nd:YAG Laser for the deposition Cu:ZnO targets were pressed under 5 tons of pressure along with a 200mJ energy pulse to prepare the pellet. 10 cm was chosen as the distance between the target and the substrate in order to heat the substrate. The slides were cleaned on glass for 15 minutes with dilated water and an ultrasonic technique Slides were wiped and dried with paper.to store the movies. Additionally, a work mask is a piece of aluminum foil the same size as the substrate (width: 2mm, spacing between electrodes: 2mm). Aluminum will be deposited using (Tungsten W) boat material these masks are placed on glass substrates and subjected to pressure (10^{-5} mbar) using a vacuum thermal evaporation technique of the Balzers-BAE370 type. Researchers occasionally alter the PLD method to improve the quality of the films created using it. The modifications include rotating the target, heating the substrate, and adjusting the substrate's position in relation to the target. The chamber is shaped like a cylinder and has a number of openings for controlling the air pressure, the substrate, and the target. The laser beam can also be controlled. The crystal structure and form were examined using atomic force microscopy (AFM). The square root rate of the surface roughness, particle size, and roughness rate were all calculated. This study examined the structure of thin films made on glass bases by recording the X-ray intensity emitted from the samples. The X-ray diffraction pattern was captured by means of XRD-6000 with CuKα (λ=1.5406A°) that have an accelerating voltage of (220/50)HZ which the SHIMADZU business manufactures,Additionally, the optical properties of the nanostructure, such as UV spectroscopy (ultraviolet spectroscopy) was used to investigate the refractive index, extinction coefficient, and real and imaginary components of the dielectric constant In the following are the most important results measurements.

Results and discussion

Structural properties

X-ray diffraction (XRD)

Figure. 1 Shows the diffraction of X-rays spectra of zinc oxide, and copper prepared by pulsed laser deposition (XRD). For the study of crystal structure, crystal size and distance between crystal levels for films Cu:ZnO and their various combinations X-ray neutralizations had been determined by using pulse laser deposition technology. (PLD) under vacuum (P = 2.5×10^{-2}mbar) and with preparation conditions included room temperature and a 200mJ laser card. YAG wavelength

1064nm The crystalline structure and size were investigated using X-ray diffraction analysis, distance between crystalline planes, and knowledge of the locations of the peaks for the films of the copper-doped compound with different ratios. the crystal size of the samples was calculated using the Debye - Scherer equation[10]:

$$D_{av} = \frac{K\lambda}{\beta \cos\theta} \ldots\ldots\ldots\ldots\ldots\ldots\ldots\ldots (١)$$

the distance between crystal levels was also determined using Brac's law of equation [10]:

$$n\lambda = 2d_{hkl} \sin\theta \quad \ldots\ldots\ldots\ldots\ldots\ldots\ldots (2)$$

where denotes the radial angle scale's full width at half-maximum peak (FWHM), expressed in units, (XRD) pattern of composite nanostructure, represents Bragg's angle, and represents the X-ray wavelength = (0.15406) nm. The pattern shows peaks for both ZnO and Cu, confirming the presence of both minerals. In this work, the growth process of ZnO and Cu nanostructures and their composite nanostructures are detailed. This sample has a collection of peaks that depict the structure of the depositing membrane at angles of and the appearance of crystalline levels at those peaks when 5% of Cu where the results showed that it has a multi-crystalline structure. Figure.1shows the X-ray diffraction spectra when 10% of Cu was added results showed that it has a multi-crystalline structure and this sample contains a group of peaks representing the structure of the depositing film at angles and the emergence of crystalline levels at those peaks, Also Figure.1 the diffraction of X-rays (XRD) spectra by adding 15% of Cu, where the results showed that it has a multi-crystalline structure and that contains peaks.

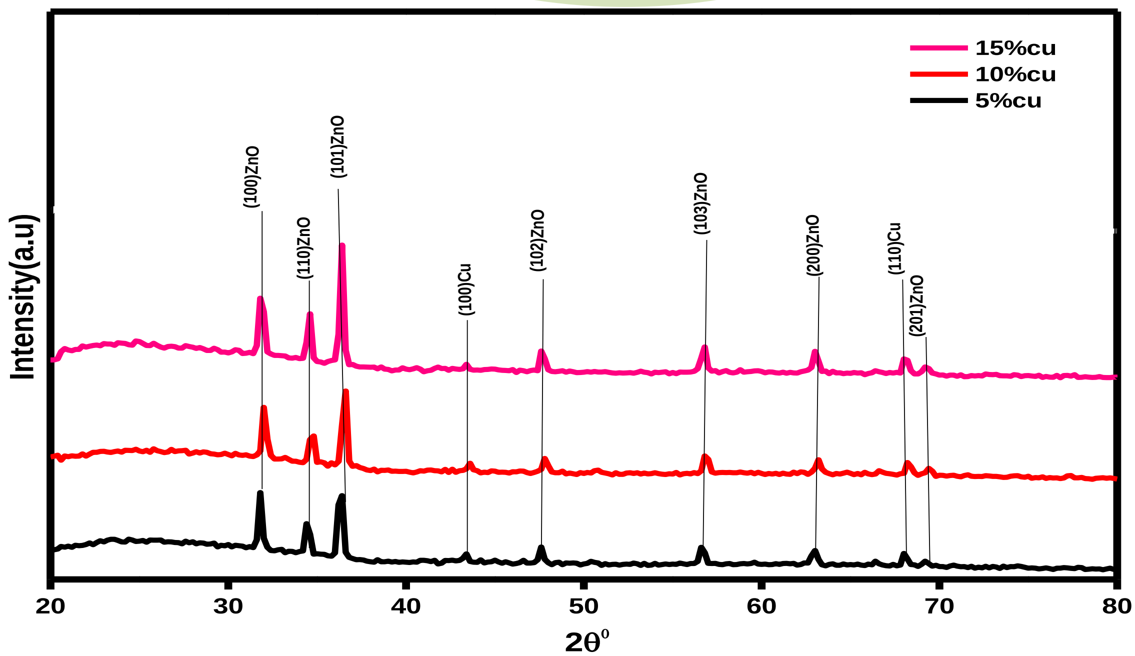

Figure.1: XRD spectra of the Cu: ZnO films generated by PLD for 5%, 10%, and 15% of Cu.

Atomic Force Microscopy (AFM)

An atomic force microscope (AFM) was used, which is type Scanning Probe Microscope SPM, model tip NsC35 / AIBSAA3000 Probe ,made in America. The device was applied to look at the topography deposited thin films on glass slides at a temperature images of Cu and ZnO films formed by a glass layer with a thickness of 250 nm are shown in Figure.2 (5%, 10%, and 15% of Cu). They were discovered to form semi-spherical clusters with equal grain sizes and to have a smooth surface as well as excellent adherence to the glass basis. The nanostructure surface benefits from an increase in corrosion percentage, and when copper ratios fall, this causes the grain size to grow [11]. The existence of a bigger nanostructures with smaller grains than the ZnO and Cu films is what causes the roughness to rise as the copper ratios increase [11]. The ZnO and Cu films nanostructures. There were provided values for average particle size, surface roughness, and root mean square. in Table.1 From the topographic images of ZnO:Cu films These results are consistent with the measured crystalline size values from X-ray diffraction and that atomic force microscopy deals with more grain size than can be monitored from X-ray diffraction In all cases, the small measured values indicate the smoothness of the surface. And the smallest particles.

5%Cu

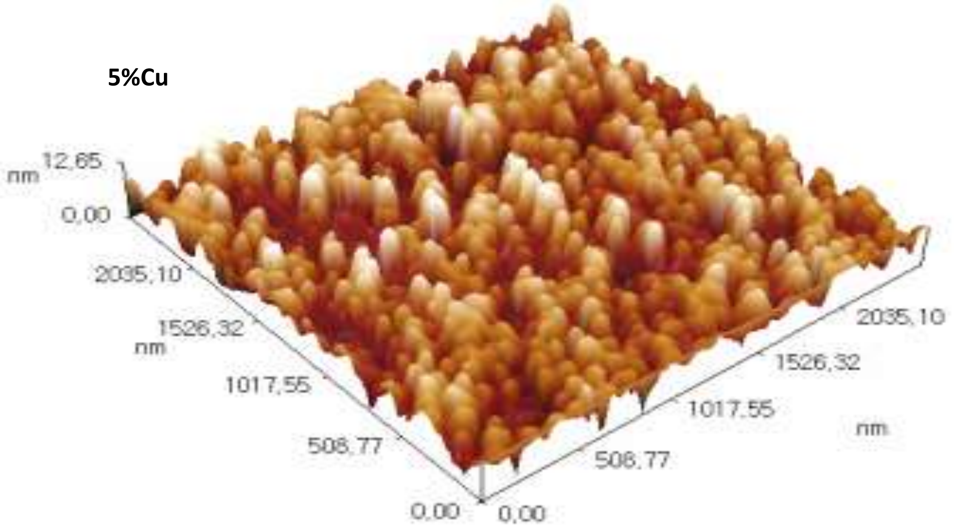

10%Cu

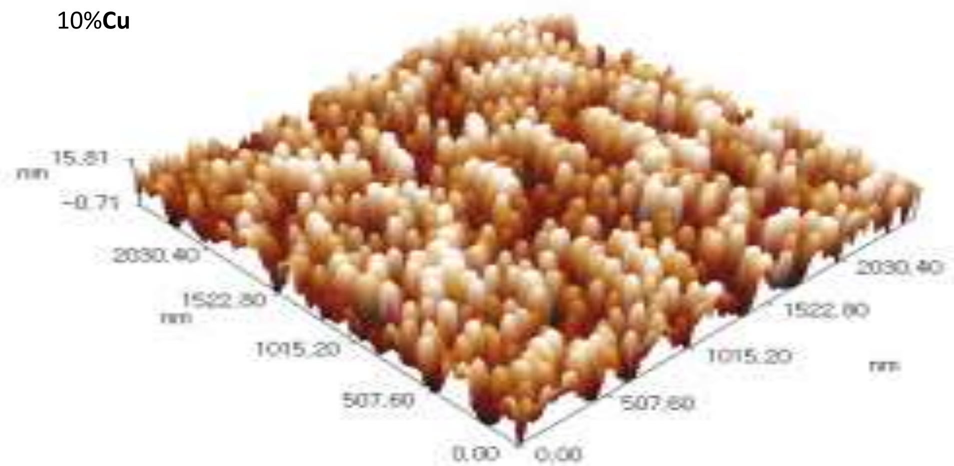

15%Cu

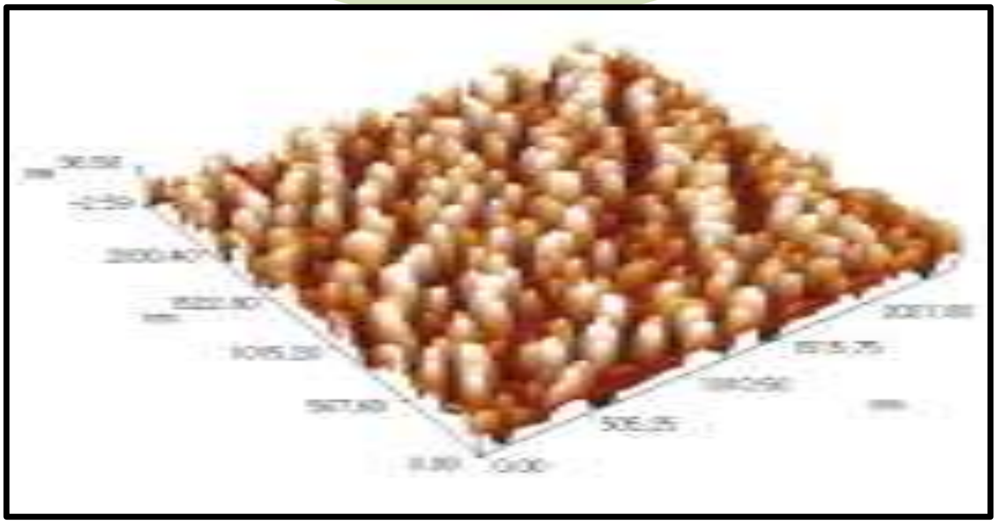

Figure.2: Topographical images of Cu:ZnO films.

Table.1 lists the Cu:ZnO films' AFM parameters.

Sample	Grain size (nm)	Ave. Roughness (nm)	Root Mean Sq. (nm)
5%Cu	51.65	2.31	2.52
10%Cu	66.78	4.51	4.78
15%Cu	86.49	6.34	7.32

Optical properties

Cu:ZnO nanocoposite which was produced on glass substrates utilizing pulse laser deposition technology at ambient temperature, are examined in this study utilizing UV-Vis spectroscopy:

The absorbance spectrum (A)

Figure.3 shows that when the amount of Cu increases, the absorption spectra will also increase. deposition of wavelength-dependent absorbance in different ZnO. In the UV region, the greatest absorption peak is located at 5% of Cu. The viewable zone is where the absorption starts to decrease. This behavior demonstrates the possibility of a short-wavelength interaction between the input photon and the material, leading to photon absorption by the substance and changes Particles of matter are found between the inner beams of the matter. the nanoparticles' vibrational states [12]. As the wavelength grows, however, the photon loses its ability to interact with the atoms of the substance. It has been noted that a rise in cu content causes the surface to become rougher.

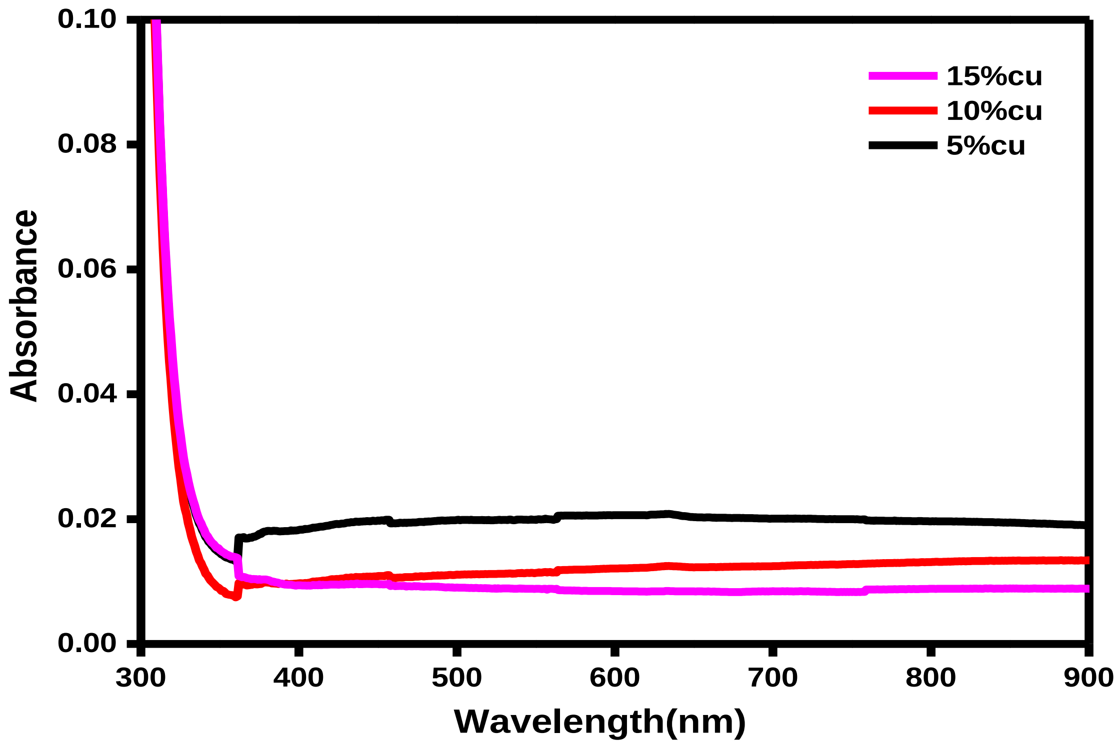

Figure.3: Deposition of absorption of Cu: ZnO films according to wavelength.

The transmission spectrum (T)

Figure.4 shows how the transmittance spectrum varies with ZnO nanocoposite wavelength. It should Please take mind that the ratio of Cu increases, the transmittance decreases. The infrared spectrum is where optical transmittance rates are at their highest, and it was found that all ZnO nanocomposite materials made using With PLD technology, optical transmittance was at its highest values at long wavelengths within the VIS-NIR ranges, a transmittance of or greater. However, the transmittance in both the films' as-deposited and annealed states shows an exponential increase from the UV to the NIR. Film is an excellent material for coating eyeglasses because of the film sample deposit's characteristics, which include poor transmittance in the UV-VIS but moderately high transmittance in the VIS-NIR. UV radiation protection from sunburn. All films' transmittance has dramatically decreased, which is attributable to the area's transparent films' absorption.

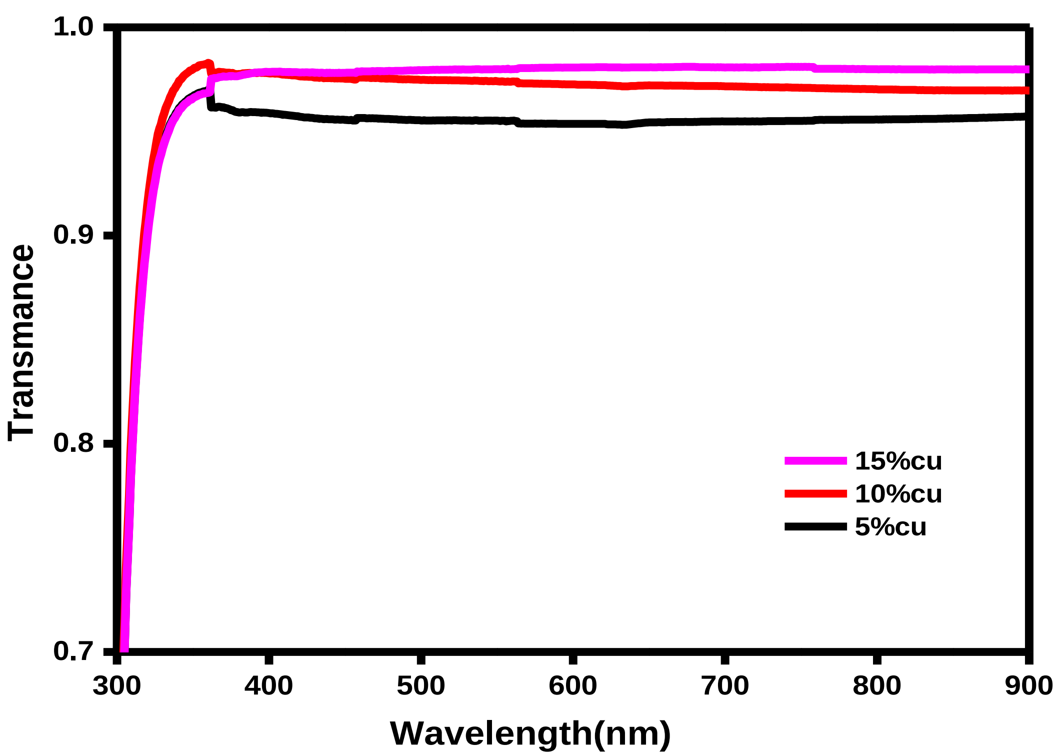

Figure.4: Transmittance of Cu: ZnO films deposited according to wavelength.

Absorption coefficient (α)

The absorption coefficient is a measure of how much radiation energy is absorbed at each unit of distance. The absorption factor is calculated using the calculation shown below [12]:

$$\alpha = \frac{2.303 * A}{t} \qquad \text{.......................................} \quad (3)$$

where t is the film thickness. As a result, depending on the wavelength, the nanostructure modifies. Figure.5 shows the relationship between the absorption coefficient and wavelength for thin Cu:ZnO films. The films absorption coefficient is shown to when they get closer to their wavelength. due to an increase in copper concentration, increasing particle size improved absorption. The photon has its most energy here since it has a narrow the direct transmission type's spectrum of wavelengths, which is where photons are most heavily absorbed.

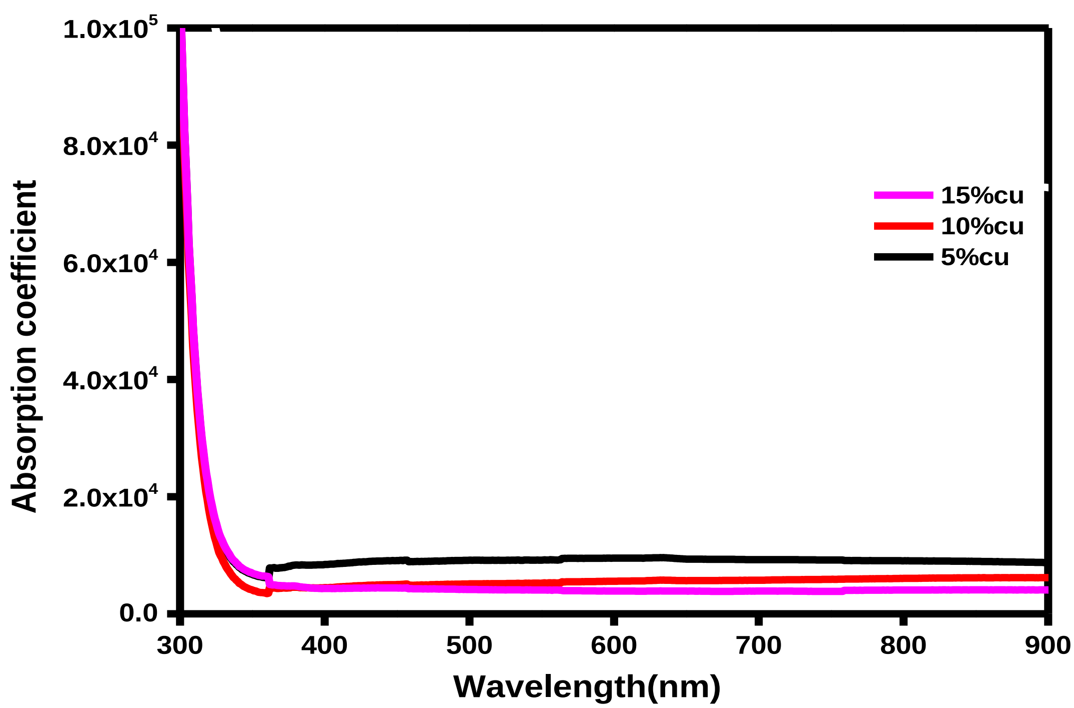

Figure.5: Absorption coefficient α of Cu: ZnO films deposited according to wavelength.

Reflectance

The following equation was used to obtain the reflectivity (R) [13]:

$$R= 1-T-A \quad \ldots\ldots\ldots\ldots\ldots\ldots\ldots\ldots\ldots\ldots\ldots\ldots\ldots \quad (4)$$

where (A) this absorption. demonstrates the thin film's wavelength-dependent reflectance spectrum. After the reflectivity values of the Cu: ZnO films at different copper were obtained when the values of the three samples prepared using the pulsed laser deposition (PLD) technique were obtained. The figure displays that coefficient (α) increases with the Cu. This behavior shows a relationship between a narrowing of the energy gap and copper. From figure this, the absorption, as well as the reflectivity was calculated through the above equation depending on the spectra of transmittance and absorption within the range of wavelengths, where we note through measurements that the reflectivity it increases at short wavelengths and then decreases gradually with increasing wavelengths.

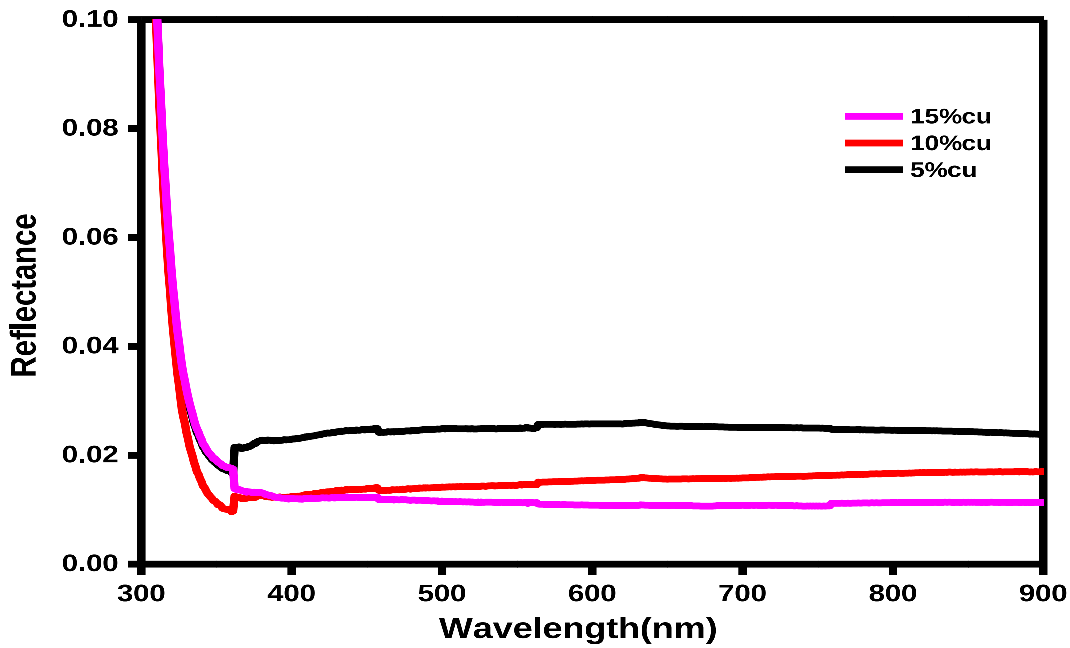

Figure.6: Reflectivity R of Cu: ZnO films deposited as a function of wavelength.

Optical energy gap (Eg)

One of the crucial optical constants in semiconductor physics is the optical energy gap, determines that semiconductors are used in electrical and optical applications[13]. The energy gap value is influenced by the crystal structure of the material. Using the absorption coefficient's value and the incident photon's energy, and its value may be determined [13]:

$$(\alpha h\nu) = A(h\nu - E_g)^r \quad \ldots\ldots\ldots\ldots\ldots\ldots\ldots\ldots\ldots\ldots\ldots\ldots\ldots\ldots (5)$$

The films in Figure.7 that were produced on glass slides with particular ratios allowed for the measurement of the energy gap. It has been found that it fluctuates in value. As the amount of copper rose, the energy gap values decreased. The maximum number of grains were visible on the surface, and this reduction demonstrates that the size of the particles in the substance has risen as a result of agitation inside the energy gap of secondary levels. The results of the visual examinations showed the occurrence of one type of basic electronic transitions, which is the direct electronic transitions, through which the value of the optical energy gap was found through an equation using the Tauc model [13]. The value of the optical energy gap was determined by graphically representing the linear relationship and selecting the best tangent line for the straight part of the curve to cut the photon energy axis, where the value of the energy strength represents the optical energy for direct transitions, demonstrating that the least amount of energy is needed to move the electron from the top of the valence band to the bottom of the conduction band. The permitted point of intersection with the photon's energy axis, where we observe that the optical energy gap's value increases as the photon's energy increases, is constrained between 2.8 and 3.2eV.

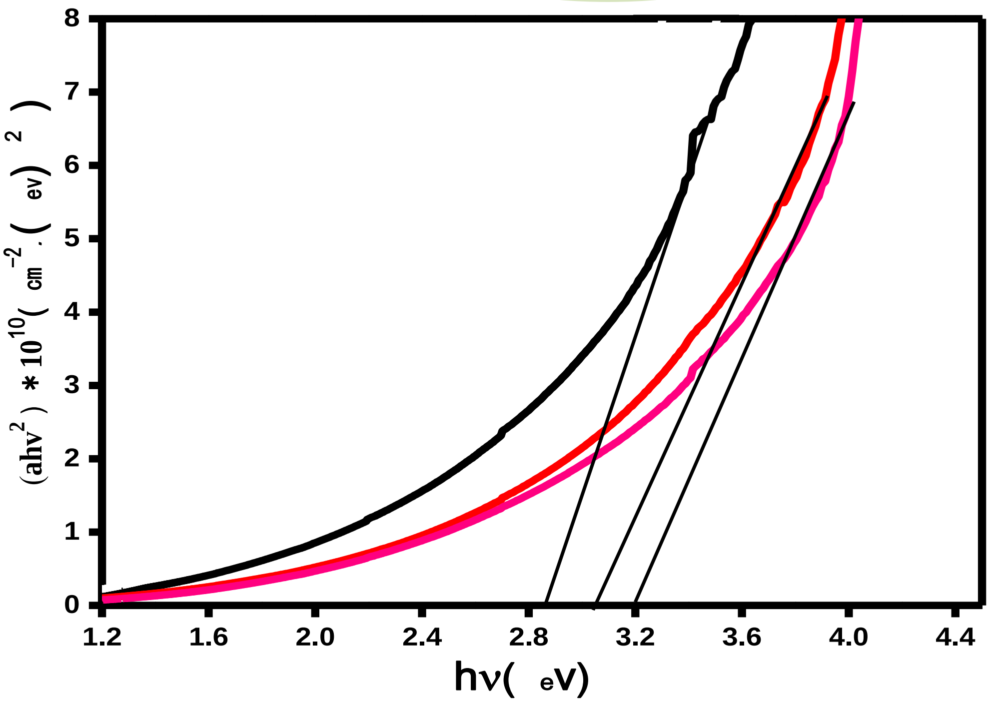

Figure.7: $(\alpha hv)^2$ being prepared Cu: ZnO films as a function of the photon energy at different Cu ratios.

Refractive index (n)

The refractive index (n) value is obtained using an equation using the extinction and reflection coefficients (K_o)[14]:

$$R = \frac{(n-1)^2+K_0^2}{(n+1)^2+K_0^2} \quad (6)$$

In the frequency range where the films absorb K_0 (n-1) and where n is the refractive index, the following equation is true [14]:

$$n = \frac{(1+\sqrt{R})}{(1-\sqrt{R})} \quad (7)$$

From figure.8 it was found that the refractive index dropped with increasing wavelength as the copper ratio rose. After being calculated using the pulsed laser deposition (PLD) process, the refractive indices of the films used in the study were determined, The equation, which was created by drawing the graphic relationship The relationship seen in the figure between the refractive index and wavelength, was used to determine the coefficients as well. it has a high value at short wavelengths and a decreasing value at short wavelengths.

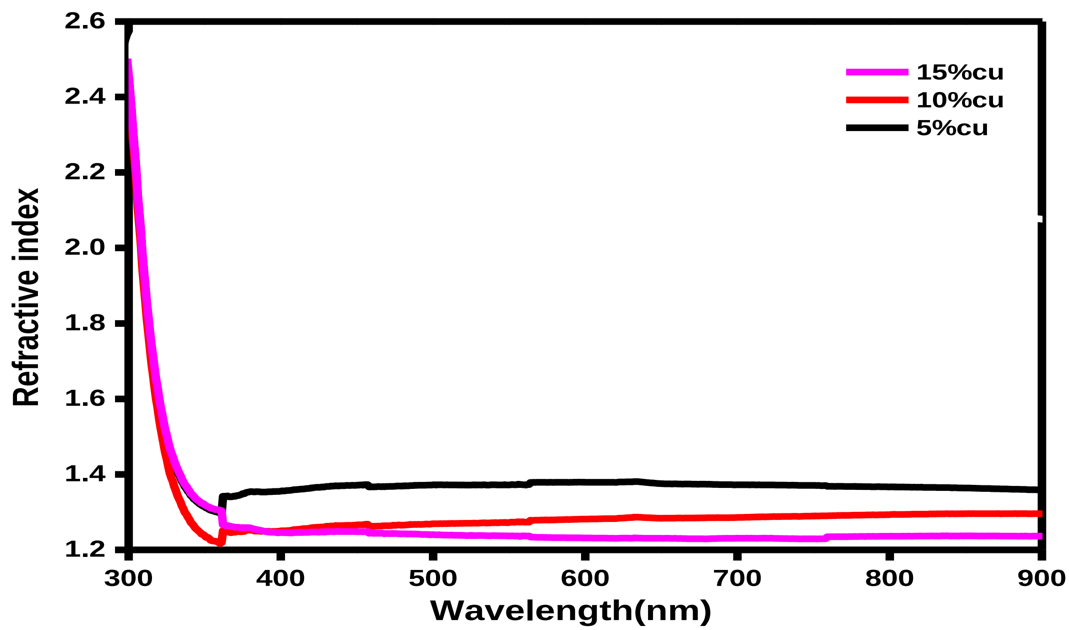

Figure.8: Refractive index (n) of Cu: ZnO films deposited according to wavelength.

Extinction coefficient (k)

A measure of extinction, which was established using the following formulae, measures energy absorbed within a nanostructure[14]:

$$K_0 = \alpha \lambda / 4\pi \quad \text{...(8)}$$

The amount of material is represented by the passivation coefficient. electrons absorbing the energy of the incoming photons, as it expresses the extent of the passivity of the electromagnetic wave within the material for the films prepared in the research. Where an equation was used to find the passivation coefficient, as it has a relationship with the absorption coefficient, so it can be calculated through the values of the absorption coefficient calculated from the absorbance spectrum of the membrane.

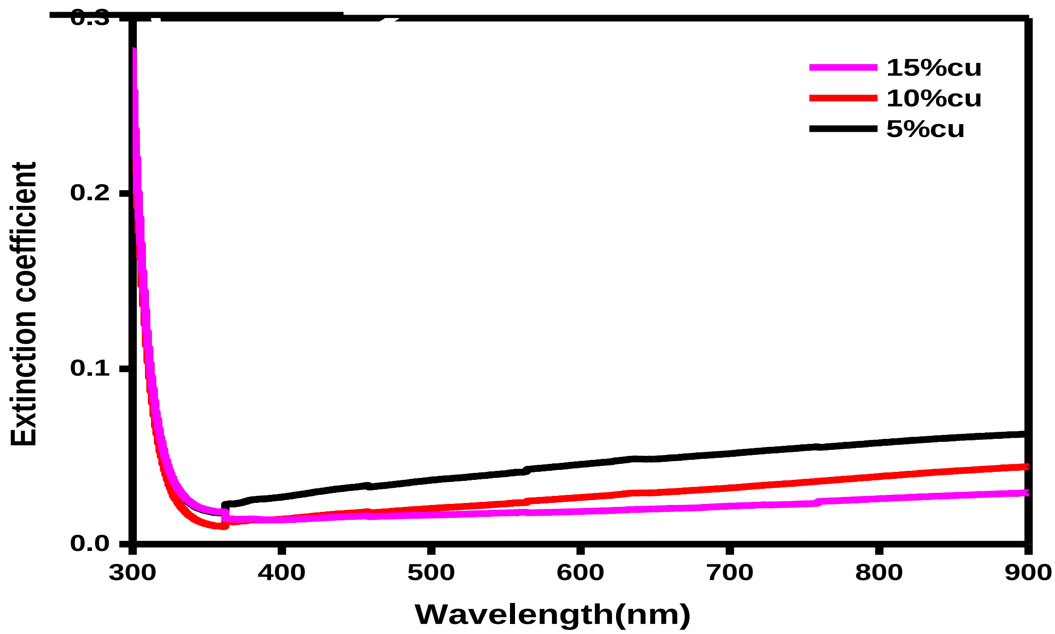

Figure.9: The Extinction coefficient (k) of Cu: ZnO films deposited according to wavelength.

Dielectric constant

based on wavelength, illustrate the difference between the real and the fictitious components of the dielectric constant. The actual and fictitious dielectric constants were computed using the following formulas [14]:

$$\varepsilon_r = n^2 - k^2 \quad \text{...}(9)$$

$$\varepsilon_i = 2nk \quad \text{...} (10)$$

This is explained by a reduction in values of the refractive index and an increase in the index of extinction values with a rise in the proportion of copper. Since the imaginary part in terms of the dielectric constant is mostly dependent on the values of the extinction coefficients, its value increased as the copper ratio did. The graphical relationship with respect to the wavelength, of the imaginary portion of the dielectric constant, as we notice that the values of the dielectric constant increase at short wavelengths, i.e. high photon energies, and decrease at long wavelengths.

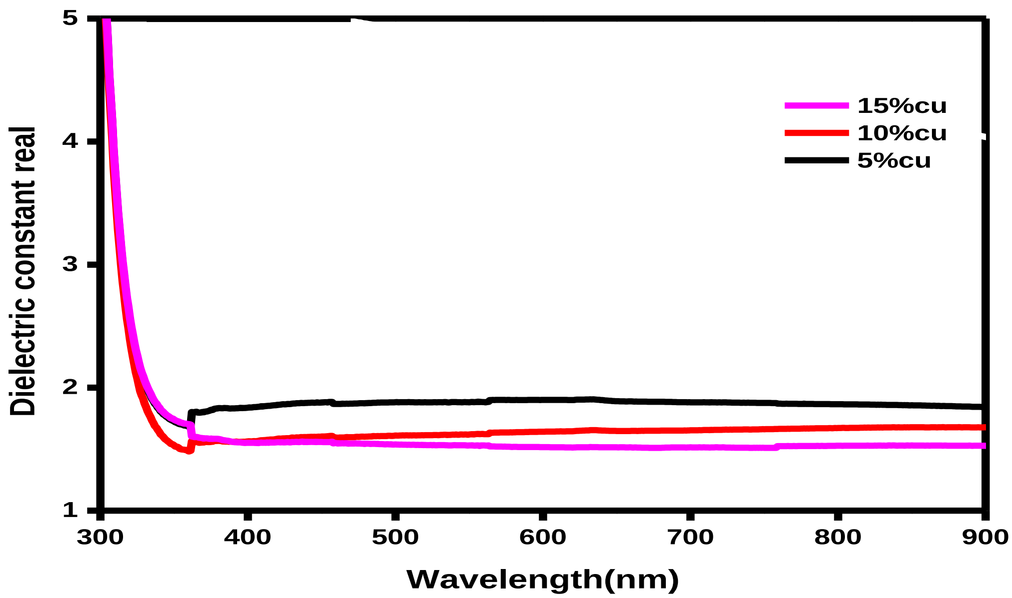

Figure.10: The dielectric constant real part (ε_r) of Cu: ZnO films with wavelength.

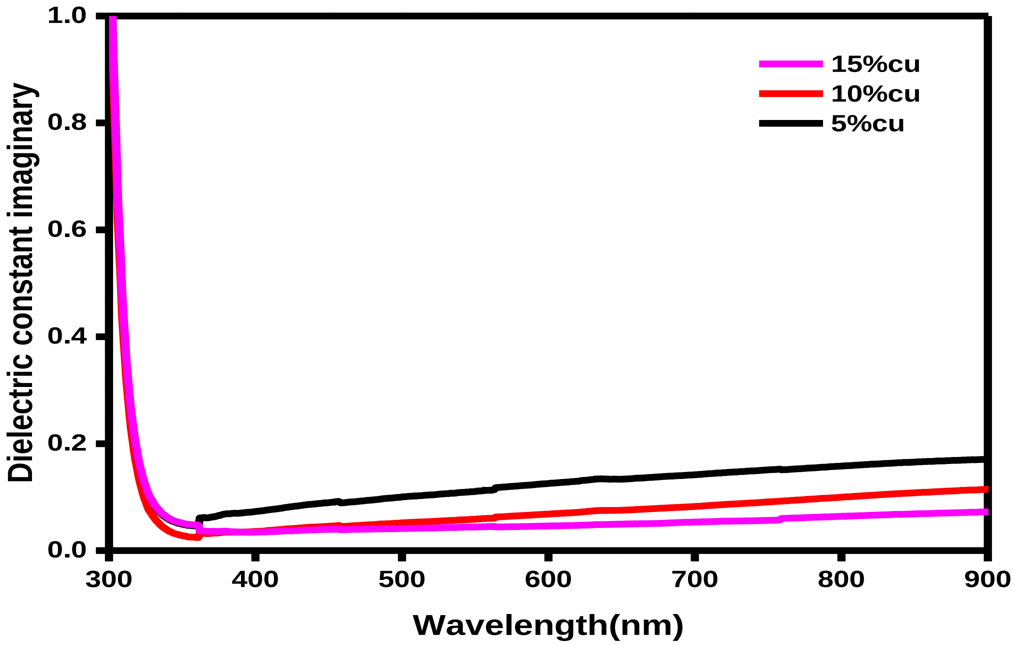

Figure.11: The dielectric constant imaginary part (ε_i) of Cu: ZnO films with wavelength.

Conclusion

The three manufactured samples in this study were measured, and an X-ray diffraction test was performed, which revealed that the samples had a nanostructure and are polycrystalline in nature. According to the atomic force microscopy findings, grain size increases as copper content rises. Additionally, shown this energy gap narrows with an increase in the amount of copper,

Acknowledgements

The acknowledgments for the every, Wasit University, Plasma Lab. Also, I thank everyone who contributed to this research, especially the group of tests needed in the research. I thank my family members for their help in preparing the research.

References

[١] Y. Matsumoto, "Energy positions of oxide semiconductors and photocatalysis with iron complex oxides," Journal of solid state chemistry, vol. 126, pp. 227-234, 1996.
[٢] M. N. Ashfold, F. Claeyssens, G. M. Fuge, and S. J. Henley, "Pulsed laser ablation and deposition of thin films," Chemical Society Reviews, vol. 33, pp. 23-31, 2004.
[٣] P. M. Monk, R. J. Mortimer, and D. R. Rosseinsky, Electrochromism and electrochromic devices vol. 421: Cambridge University Press Cambridge, 2007.
[٤] K. Chopra, Thin film device applications: Springer Science & Business Media, 2012.
[5] E. Cagin, "Integration Of Functional Oxides With The Semiconductor Zinc Oxide," 2010.
[٦] C. Jagadish and S. J. Pearton, Zinc oxide bulk, thin films and nanostructures: processing, properties, and applications: Elsevier, 2011.
[٧] Z. C. Feng, Handbook of zinc oxide and related materials: volume two, devices and nano-engineering: CRC press, 2012.
[٨] J. Zhong, A. H. Kitai, P. Mascher, and W. Puff, "The influence of processing conditions on point defects and luminescence centers in ZnO," Journal of the Electrochemical Society, vol. 140, p. 3644, 1993.
[٩] V. Parthasarathi and G. Thilagavathi, "Synthesis and characterization of zinc oxide nanopartilce and its application on fabrics for microbe resistant defence clothing," International Journal of Pharmacy and Pharmaceutical Sciences, vol. 3, pp. 392-398, 2011.
[١٠] T. H. Mubarak, K. H. Hassan, and Z. M. A. Abbas, "Using X-ray diffraction and scanning electron microscope to study zinc oxide nanoparticles prepared by wet chemical method," in Advanced Materials Research, 2013, pp. 119-122.
[١١] A. Yousif, "Characterization of ZnO Film Grown on Different Substrates Using PLD," Ph. D Thesis, University of Technology Department of Applied Science, 2, 2010.
[12] M. Willander, Zinc oxide nanostructures: advances and applications: CRC Press, 2014.
[13] A. Barchanski, Laser-generated functional nanoparticle bioconjugates: design for application in biomedical science and reproductive biology. Springer, 2016.
[14] S. S. Harilal, C. V. Bindhu, M. S. Tillack, F. Najmabadi, and A. C. Gaeris, “Internal structure and expansion dynamics of laser ablation plumes into ambient gases,” J. Appl. Phys., vol. 93, no. 5, pp. 2380–2388, 2003, doi: 10.1063/1.1544070.